Toward Efficient Binders for Li-Ion Battery Si-Based Anodes: Polyacrylic Acid

Alexandre Magasinski,[†] Bogdan Zdyrko,[‡] Igor Kovalenko,[†] Benjamin Hertzberg,[†] Ruslan Burtovyy,[‡] Christopher F. Huebner,[†,§] Thomas F. Fuller,[∥] Igor Luzinov,[*,‡] and Gleb Yushin[*,†]

School of Materials Science and Engineering and School of Chemical & Biomolecular Engineering, Georgia Institute of Technology, Atlanta, Georgia, United States, School of Materials Science and Engineering, Clemson University, Clemson, South Carolina, United States, and Streamline Nanotechnologies Inc., Atlanta, Georgia, United States

ABSTRACT Si-based Li-ion battery anodes offer specific capacity an order of magnitude beyond that of conventional graphite. However, the formation of stable Si anodes is a challenge because of significant volume changes occuring during their electrochemical alloying and dealloying with Li. Binder selection and optimization may allow significant improvements in the stability of Si-based anodes. Most studies of Si anodes have involved the use of carboxymethylcellulose (CMC) and poly(vinylidene fluoride) (PVDF) binders. Herein, we show for the first time that pure poly(acrylic acid) (PAA), possessing certain mechanical properties comparable to those of CMC but containing a higher concentration of carboxylic functional groups, may offer superior performance as a binder for Si anodes. We further show the positive impact of carbon coating on the stability of the anode. The carbon-coated Si nanopowder anodes, tested between 0.01 and 1 V vs Li/Li+ and containing as little as 15 wt % of PAA, showed excellent stability during the first hundred cycles. The results obtained open new avenues to explore a novel series of binders from the polyvinyl acids (PVA) family.

KEYWORDS: Li-ion • anode • Si • nanopowder • polyacrylic acid • binder

INTRODUCTION

Si-based Li-ion battery anodes have recently attracted noteworthy attention, as they offer specific capacity an order of magnitude beyond that of conventionally used graphite (1−5). However, high-capacity Si particles exhibit large volume changes during Li insertion and extraction. This expansion and contraction during the operation causes significant challenges in selecting the binder, which holds the active material together in the anode of a Li-ion battery. The most conventional binder (poly(vinylidene fluoride), PVDF) used for the batteries is attached to Si particles via weak van der Waals forces only, and fails to accommodate large changes in spacing between the particles. It rapidly becomes inefficient in holding the particles together and maintaining electrical conductivity within the anode, which is required for battery operation (6−9). Development of more efficient binders is therefore an important task for the realization of stable high capacity anodes.

Until now, most studies were focused on the modification and use of PVDF or carboxymethylcellulose (CMC)-based binders (10−17). For example, heat treatment of PVDF-based Si anodes in argon at 300−350 °C (16) or cross-linking a PVDF-based Si−Sn anodes (17) was found to increase the binder elastic modulus and strength and simultaneously improve anode stability.

Significant amounts of data have been gathered for CMC binders, which typically demonstrate a better performance and can be considered to be the state of the art in this field. For example, Chen et al. proposed to use a commercial adhesive and its mixture with sodium carboxymethylcellulose (Na-CMC) (2:1) for C/nano-Si anodes (10)]. A capacity of 500 mA h/g with less than 20 % degradation was achieved for 50 cycles. The addition of Na-CMC was found to favorably affect the performance of the binder. Liu et al. studied a mixture of commercial butadiene block copolymer (SBR) latex and Na-CMC (1:1) as a binder for C/Si anodes, with high Si (62 wt.%) and moderate binder (8 wt %) content (11). The Si particles were milled to 1−3 μm and coated with a thick C layer (30 wt %). They observed major improvements in electrode capacity and stability when SBR was used. Under constant lithiation to 1000 mA h/g, the electrodes demonstrated very stable performance for 50 cycles. Buqa et al. also investigated Na-CMC and SBR mixture (1:1) as binders for C/nano-Si composite anodes prepared by direct mixing (Si:C ≈ 1:9) (12). They observed reasonably stable performance of electrodes for up to 150 cycles, with the discharge capacity decreasing from 700 to 550 mA h/g. The binder content was only 5 and 2 wt % in the case of the Na-CMC and SBR/Na-CMC mixtures, respectively. The effects of larger binder content were not studied, because of the expectation that it might hinder diffusion of Li+ ions.

Li et al. compared the performance of Na-CMC and SBR/Na-CMC (1:1) binders for macroscopic (8 μm, 325 mesh) Si powders with conductive additives (Si:C:binder = 80:12:8)

* Corresponding author. E-mail: luzinov@clemson.edu (I.G.); yushin@gatech.edu (G.Y.).

Received for review February 16, 2010 and accepted October 20, 2010

[†] School of Materials Science and Engineering, Georgia Institute of Technology.
[‡] Clemson University.
[§] Streamline Nanotechnologies Inc.
[∥] School of Chemical & Biomolecular Engineering, Georgia Institute of Technology.

DOI: 10.1021/am100871y

(13). In order to minimize anode degradation, they limited the lower potential to 170 mV (vs Li/Li+). The pure CMC binder demonstrated better performance, with electrode deintercalation capacity decreasing from 1600 to 700 mA h/g (~56%) after 80 cycles. Interestingly, one of the CMC electrodes showed oscillating behavior, with the specific capacity changing between 1300 and 1100 mA h/g during 70 cycles. Key et al. suggested an improved long-term stability of electrolyte against continuous decomposition on the Si surface upon cycling, when Si particles are protected with CMC (18). Beattie et al. suggested using considerably higher Na-CMC binder content (up to 70%) in order to provide space for Si to expand during Li insertion (14). Anodes containing 20 wt % Si and 70 wt % Na-CMC exhibited only 25% capacity fading between the third and 200th cycle. However, the overall anode capacity was below 400 mA h/g because of the low content of active material. Anodes with higher Si and C and lower binder content (33 wt % Si, 33 wt % C, and 33 wt % binder) showed significantly higher initial capacity (1200 mAh/g), but faster capacity fading (25% in 25 cycles). A follow-up study of the same group showed further improved stability of the anode with this optimum composition (Si:C:binder = 1:1:1) and proposed that hydrogen bonding between carboxy groups in CMC and hydroxyl groups on Si surface exhibits self-healing behavior that allows for the long-term cycling stability (19). In recent studies Mazouzi et al. achieved a very impressive 700 cycles when they optimized the pH of the Na-CMC binder solution to enhance the strength of Si-binder interaction and minimized the stresses and volume changes in Si by employing Li insertion capacity limited to 960 mAh/g, about one-third of the full Si capacity (15).

Whereas Na-CMC shows reasonable performance with Si anodes, it suffers from several limitations. First, Na-CMC is not soluble in organic solvents. While the use of water as a solvent is advantageous for the environment, it causes the surface oxidation of Si and may affect the Columbic efficiency and long-term stability of Si-based anodes. Second, while CMC-Si anodes can be improved (15, 20), the mechanical properties of CMC are fixed, and therefore cannot be optimized for Si anodes. This may potentially explain why good Si/Na-CMC anode stability is commonly achievable only when Si volume changes are minimized via a limited Li insertion capacity (12, 15). Finally, the molecular weight of Na-CMC derived from natural cellulose is impossible to regulate. Surprisingly, other binder chemistries have received relatively little attention.

In this manuscript, we report on the use of poly(acrylic acid) (PAA) as an advanced binder for Si-based anodes, which offers improved anode stability, tunable properties and other attractive attributes. Although PAA (PAA salt) binders have been used for C (21) and Sn−Co−C anodes (22), successful application of PAA for Si anodes has never been reported. Similar to other members of the polyvinyl acids (PVA) family (23), PAA is soluble not only in water but also in a variety of ecologically friendly organic solvents, such as ethanol. PAA (or PVA) binders offer a much higher concentration of functional groups and allow one to control the effective spacing between them via copolymerization with other monomers. The copolymerization also allows for varying binder mechanical properties as well as swelling and solubility in an electrolyte solvent. It is also possible to obtain acrylic acid containing polymers with block and graft copolymer architecture. This flexibility in solvent selection, precise control over the distribution of functional groups and the tunable mechanical properties of such binders provide new degrees of freedom for the electrode preparation and optimization processes. In addition, PAA (or PVA)-based binders may serve as a good model system for performing systematic studies of the effects of binder properties (elastic modulus, maximum elongation, swelling in electrolyte, surface chemistry, the binder-Si or binder-C bond, the strength of the adhesion between the electrode components and others) on the performance of the Si anode. In the present paper, we report the results obtained using pure PAA as an anode binder. The performance of other PVA binders, including the copolymerized ones, will be reported separately.

EXPERIMENTAL SECTION

Si nanopowder was purchased from Hefei Kaier Nanotechnology Development Co., China. The sample had a very high content of SiO_2 (up to 70 wt % according to energy dispersive spectroscopy (EDS) studies). To remove the majority of the SiO_2, all powders were purified using a 50% HF solution. Selected HF-cleaned Si powder samples were then coated with carbon. For this purpose, Si nanoparticles were first dispersed in tetrahydrofuran (THF) using an ultrasonic bath (Branson, USA) and thoroughly mixed with polycarbonate (PC) (M_w = 64,000 g/mol, Sigma-Aldrich, USA) solution in THF under continuous flask rotation (100 rpm). The THF solvent was then slowly replaced with ethanol, causing the formation of a uniform PC coating on the powder surface. The PC-coated Si was then separated from the solvent using a high speed centrifuge (5000 rpm, Fischer Scientific, USA) and annealed under Ar flow (50 sccm) for 2 h at 800 °C to induce the graphitization of the PC.

Scanning electron microscopy (SEM) and EDS studies were performed using a LEO 1530 SEM microscope (LEO, Japan, now Nano Technology Systems Division of Carl Zeiss SMT, USA). An in-lens secondary electron detector was used for the imaging. Most of the micrographs were recorded at an accelerating voltage of 6 kV and a working distance of 5 mm.

PAA (M_w = 2000, 5000, and 100 000 g/mol) was purchased from Sigma-Aldrich, USA. PAA with M_w = 100 000 g/mol dissolved in ethanol was used as a binder. PVDF in N-Methyl-2-pyrrolidone (NMP) (9305, Kureha, Japan) and Na-CMC (M_w = 500 000 g/mol, substitution degree =0.9, Alfa Aesar, USA) in H_2O with the addition of ethanol (5 wt %) were used as alternative binders, for comparison. For consistency, all electrodes contained approximately 15 wt % of the binder, 43 wt % of Si and 42 wt % of C, either as conductive additives (high temperature annealed carbon black, PureBlack, produced and supplied by Superior Graphite, USA) or as a combination of a surface coating (17 wt %) and additives (25 wt %). The electrode slurries were thoroughly mixed using an ultrasonic bath and a laboratory stirrer (600 rpm) for at least 1 h, cast on a 18 μm Cu foil (Fukuda, Japan) using a 150 μm doctor-blade, dried in air first at room temperature and then at 60 °C for at least 4 h, degassed in vacuum at 70 °C for at least 2 h inside an Ar-filled glovebox (<1 ppm of oxygen and water, Innovative Technology, Inc., USA) and were not exposed to air prior to their assembly into the cells. The commercial electrolyte was composed of 1 M $LiPF_6$ salt in ethylene carbonate-diethyl carbonate-dimethyl

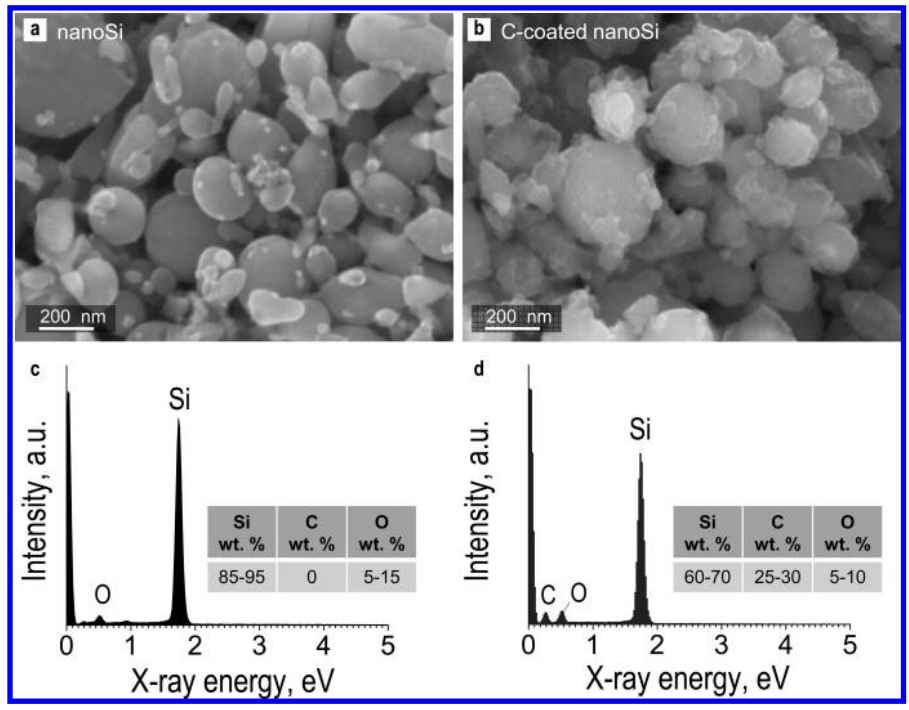

FIGURE 1. SEM micrographs and EDS spectra of HF-cleaned Si nanopowder (a, c) before and (b, d) after carbon coating.

carbonate mixture (EC:DEC:DMC = 1:1:1 vol %) (Novolyte Technologies, USA). For long-term cycling tests we have added five wt % vinylene carbonate (VC) (Alfa Aesar, USA) into the electrolyte solution. Lithium metal foil (0.9 mm thick, Alfa Aesar, USA) was used as a counter electrode. 2016 stainless steel coin cells were used for electrochemical measurements. The Cu current collector of the working electrode was spot-welded to the coin cell for improved electrical contact. Charge and discharge rates were calculated assuming the experimentally determined capacity for C and the maximum theoretical capacity for Si (4200 mA h/g), given the composition of the active material (either C or C−Si mixture). Long-term cycling was performed in the range of 0.01−1 V vs Li/Li$^+$. Coulombic efficiency was calculated as100 % · ((C^{dealloy})/(C^{alloy})), where C^{alloy} and C^{dealloy} are the capacity of the anodes for Li insertion and extraction. Arbin SB2000 (Arbin Instruments, USA) and Solartron 1480 (Solartron Analytical, USA) multichannel potentiostats were used for electrochemical measurements. The capacity of each type of C used in the Si−C anodes was determined in separate tests where anode was made with the C and a binder only. In order to demonstrate the effect of the binder on Si anode performance, the specific capacity is reported for Si contribution only (the contribution of C was subtracted from the reported results because different types of C exhibit different capacitance values). The specific capacity for the actual electrodes is roughly ∼50 % lower because of the weight of the binder and low specific capacity of C.

Swelling ellipsometry studies on thin binder films (PAA, Na-CMC, and PVDF) deposited on Si wafers were performed with a COMPEL automatic ellipsometer (InOmTech, Inc., USA) at an angle of incidence of 70°. Original Si wafers from the same batch with a native oxide layer were tested independently and used as reference samples for the swelling analysis of polymer binders in carbonates. The polymer binders were deposited on Si using a dip-coating method (dip coater, Mayer Fientechnik D-3400) to an initial thickness of 30−70 nm and were placed in a closed chamber with an open container filled with carbonate. We have selected pure DEC as a model carbonate for these experiments, since it is a liquid (EC is a solid) and has lower volatility compared to DMC. Film thickness measurements were performed until the changes in ellipsometric parameters leveled off due to equilibration of the polymer film thickness upon DEC vapor infiltration. The thickness of the polymer binder was obtained by fitting the ellipsometric data, assuming the refractive index of the binder and carbonate to be 1.5.

The mechanical properties of the binders (PAA, Na-CMC, and PVDF) were measured with atomic force microscopy (AFM) by the tip indentation technique (24). Studies were performed on a Dimension 3100 (Digital Instruments Inc., USA) microscope. Polymer films with the thickness of 1−2 μm were tested. The thicker films were needed to avoid influence of underlying substrate on the measurements. Force−distance data were collected using silicone cantilevers with a spring constant of 40 N/m with approaching-retracting probing frequency of 1−2 Hz. Force-volume measurements were used to obtain the stiffness distribution over the surface of the sample. Measurements were performed on samples in both a dry state and a "wet" state after the film was immersed into DEC. PVDF in a dry state was used as the reference and the stiffness data were normalized accordingly.

RESULTS AND DISCUSSION

Si Powder. SEM shows a rather broad particle size distribution in the Si nanopowder, with some particles as small as 20 nm and others in excess of 1 μm. However, most of the Si nanoparticles (by volume) were in the range of 100−400 nm after the HF cleaning (Figure 1a). Carbon coating was highly conformal (Figure 1b) and reasonably uniform within the powder. The amount of the deposited C was close to 25−30 wt %, according to EDS measurements (Figures 1 c, d) and estimations from the mass changes during PC deposition on the Si powder surface and its graphitization. Assuming a uniform coating formation, a perfect spherical shape of Si nanoparticles, the density of C coating to be 2.2 g/cm^3, and the density of Si nanoparticles to be 2.3 g/cm^3, we estimated the thickness of C coating to be 10−30 nm. The oxygen detected by EDS (Figure 1c, d)

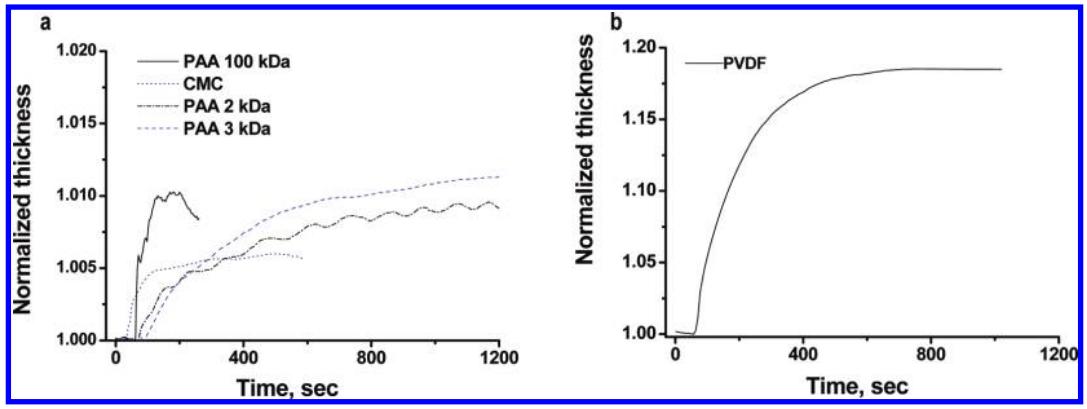

FIGURE 2. Swelling of (a) PAA with different M_w and Na-CMC, and (b) PVDF in diethylcarbonate vapor. The data were obtained by ellipsometric measurements and normalized to the thickness of an initial "dry" film.

was assumed to come from the remaining oxide layer and the physisorbed water.

Binders. The performance of a polymer binder in an anode is expected to depend on at least four parameters: (i) adhesion strength between the electrode and the current collector foil, (ii) the interface between the polymer and the active particles, (iii) interaction of the binder with the electrolyte, and (iv) binder mechanical properties. The first parameter is well-understood, because strong adhesion is definitely needed to ensure integrity of the anode. From this point of view, Na-CMC and PAA polymers are superior to PVDF, because carboxy functional groups present in the binders interact strongly with SiO_2 (present on Si particle surface) via hydrogen bonding. The polymers also can interact with copper surface via hydrogen bonding (with Cu oxide) and/or Cu salt formation. However, the optimal interface structure, the effect of interaction with electrolyte and the influence of mechanical properties are still to be determined. Where mechanical properties of the binders are concerned, PAA has the highest reported stress at break, σ_b: PAA σ_b is about 90 MPa (25), Na-CMC σ_b is reported to be 30 MPa (26), and PVDF σ_b is close to 37 MPa (27). In terms of elongation, PVDF demonstrates elongation at break above 50% (27), whereas the elongation for Na-CMC is only 6% (26). PAA is reported to demonstrate brittle fracture behavior, which indicates a low percentage of elongation.

To evaluate the level of interaction between PAA/Na-CMC/PVDF and carbonates, we measured the swellability of the polymer films in DEC vapor. Figure 2 shows changes in the ellipsometric thickness for PAA (M_w = 2000, 5000, and 100 000 g/mol), Na-CMC, and PVDF films upon exposure to carbonate vapors. Because the solubility (and swellability) of the polymer in a solvent depends on polymer molecular weight, we studied several PAA samples, including those with M_w substantially lower than the ones used in the binder. Interestingly, the swellability of all the PAA samples did not show a strong dependence on the M_w and was minute, ~1%. The negligibly small swellability of the PAA in the carbonate vapors indicates a low level of polymer/electrolyte interaction. Na-CMC film also demonstrated very low swelling in DEC. Therefore, we envision the absence of any substantial decrease in glass-transition temperature of the PAA and Na-CMC binders upon soaking in the battery

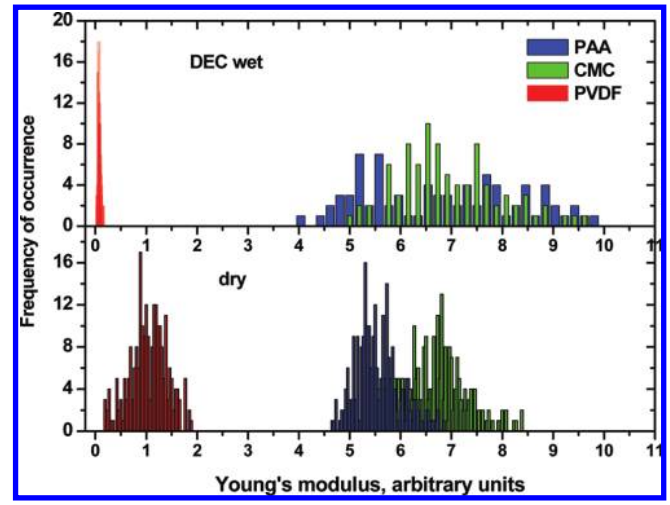

FIGURE 3. Results of AFM stiffness measurements for films made from PAA (100 000 g/mol), CMC, and PVDF. Results are normalized to stiffness of PVDF in dry state.

electrolyte. In other words, the changes in the PAA and Na-CMC resiliency or other mechanical properties upon electrolyte infiltration should be modest, if any. Conversely, PVDF films attract significant amounts of carbonate from the vapor, demonstrating changes in thicknesses of up to 20%. Therefore, a significant change in mechanical properties is expected for PVDF material in contract with electrolyte.

To confirm that the electrolyte solvent does not have a significant influence on mechanical properties of the binder under consideration, we have studied the stiffness of PAA in a dry state as well as in contact with DEC liquid using AFM tip indentation measurements. The studies were performed with PVDF and Na-CMC binders for comparison. In a dry state, PAA is significantly stiffer that PVDF (Figure 3). This result is in accord with published data on stiffness of the polymers. Specifically, Young's moduli of polymers were reported to be on the level of 4000 and 650 MPa for PAA and PVDF, respectively (25, 27). Na-CMC film demonstrated stiffness close to the one of PAA. In agreement with ellipsometry measurements, for all intents and purposes the moduli of PAA and Na-CMC do not change when exposed to DEC. In contrast, the stiffness of PVDF was significantly decreased by contact with DEC. Such experiments suggest that PVDF binder in electrolyte solution should behave as

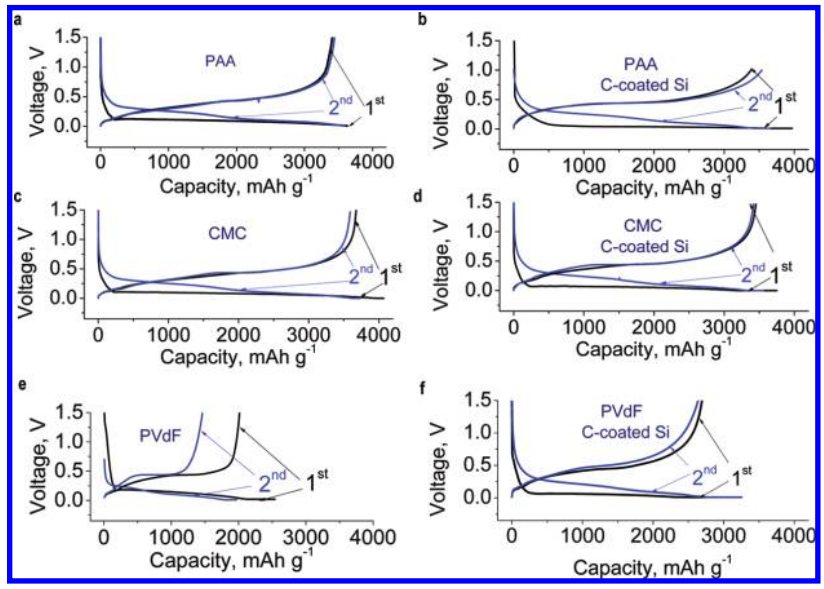

FIGURE 4. Galvanostatic charge−discharge profiles of the Si-based anodes with different binders recorded at the C/20 rate: (a, b) PAA, (c, d) CMC, (e, f) PVDF. Profiles reported for Si part of the anode only.

an easily deformable material with small resistance to both elastic and plastic deformations. While PVDF binder is known to provide stable performance to the electrodes which do not change volume upon Li insertion/extraction, the PVDF's weak resistance to deformations may explain its reported poor performance in Si anodes, which undergo large volume changes. Once deformed, PVDF largely becomes incapable of keeping Si particles in contact during their subsequent contraction.

Anode Characterization. Figure 4 shows the profiles for the first two cycles of charge and discharge of the Si anodes. The performance of the PAA binder is compared to that of Na-CMC and PVDF. Since we were primarily interested not in a long-term anode stability, but rather in an assessment of a binder performance under extreme conditions, we performed charge−discharge cycling to nearly 100% depth-of-discharge (DoD) (to 0.01 mV vs L/Li+) and did not limit the insertion capacity or the lower potential range. We also used a relatively small binder content (15 wt %) for all the tests. All anode samples show a flat plateau at low potential values during the first Li insertion. At this stage, crystalline Si nanoparticles gradually transform into an amorphous Li_xSi phase with no abrupt structural changes visible, as indicated by the absence of multiple voltage plateaus.

At about 50% capacity and about 0.4 V, the curvature of the Li extraction curve changes from negative to positive (Figure 4). The second and subsequent insertion curves also exhibit gradual voltage change with no clear plateaus. Interestingly, in contrast to micrometer-sized Si powder (28), Li insertion curves for nanoSi cover a larger potential range and reach 0.2 V or lower potentials not immediately but after ~30% Li insertion. This behavior may be related to the absence of crystalline regions in nanoSi after the first cycle (29), and results in slightly lower terminal voltage of Li-ion batteries with nanoparticle anodes. The shape of the Li insertion and extraction profiles discussed above are rather similar for all of the investigated anodes (compare Figure 4a-f) as well as curves reported in literature (14, 15, 29). The maximum reversible Li deintercalation capacity of our anodes was typically lower than 4200 mAh/g (theoretical for $Li_{22}Si_5$ phase). Several groups (30, 31) suggested that such a high degree of silicon lithiation is not possible at room temperature. However, these conclusions may be premature for nano-Si, because the relatively low extraction capacity may be related to the loss of electrical contact in a small portion of active particles upon Li_xSi contraction or to the blockage of the Li^+ ions by the binder or (in the case of nanoSi) to the presence of SiO_2.

NanoSi anodes with both PAA (Figure 4a,b) and Na-CMC (Figure 4c,d) binders commonly showed capacities close to 3300−3700 mA h/g, whereas the capacity of PVDF-based anodes was significantly lower (Figure 4e,f). The stability of the anodes during the first two cycles showed the major influence of the binder used. The capacity of both Si and C-coated Si anodes with PAA binder increased after the first cycle, suggesting that not all of the Si nanoparticles were initially active and the path of Li ions to Si was partially blocked. The volume changes likely exposed previously inactive Si to electrolyte at the second cycle. In comparison, the degradation of the anodes was moderate but clearly observed when Na-CMC binder was used, particularly when Si particles were not coated with carbon (Figure 4c). We noticed a slightly higher initial anode capacity with Na-CMC binder, particularly when bare Si powder was used (Figure 4c). This might be related to fewer carboxylic functional groups being available in Na-CMC and therefore incomplete particle coating, which allowed more nanoSi particles to be accessible for electrochemical reaction with Li. The more common PVDF binder showed the worst performance, with low capacity and rapid capacity fading, particularly when Si particles were not coated with C. We speculate that C coating may have bridged many Si particles and provided electrical connectivity within the anode for several cycles, even when

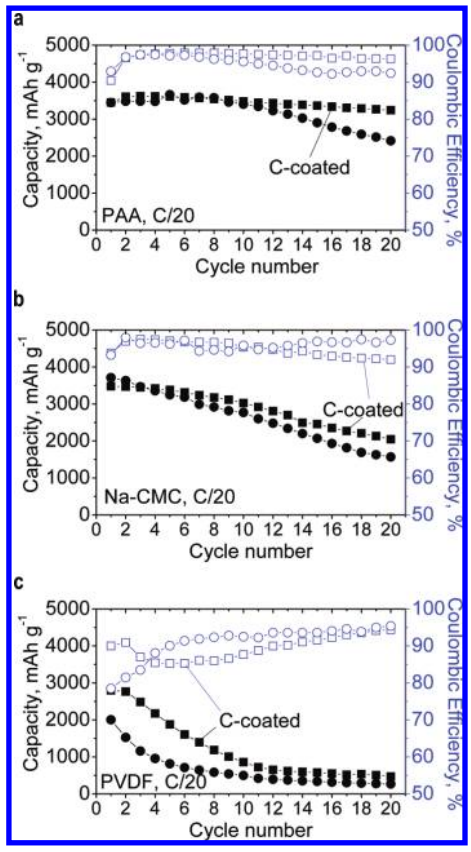

FIGURE 5. Reversible Li deintercalation capacity and Coulombic efficiency of the Si-based anodes with different binders: (a) PAA, (b) CMC, and (c) PVDF. All measurements were performed at room temperature in two-electrode 2016 coin-type half-cells. Si:C = 1:1. Capacity reported for Si part of the anode only. Square symbols correspond to anodes with Si particles coated by C.

the binder started to fail. We also speculate that the PVDF did not coat all the particles uniformly and likely blocked Li ion access to a significant portion of Si, leading to low capacity even at the first cycle.

The Li insertion and extraction capacities for the first twenty cycles are shown in Figure 5. The performance of PAA compares very favorably to the more common Na-CMC and PVDF binders. Both C-coated and bare Si anodes showed outstanding stability for the first 6−8 cycles (Figure 5a). However, longer cycles lead to the decrease in the Coulombic efficiency (CE) and, in the case of bare Si, to relatively fast degradation, suggesting the formation and propagation of microdefects and electrically isolated areas within the anode. Decrease in CE after the 6−8 cycles for both CMC and PAA-based electrodes was largely linked to the electrode degradation. We suggest that the yet unoptimized mechanical properties of the pure PAA binder and unoptimized bonding between PAA and Si are at least partially responsible for the eventual anode failure. Interestingly, carbon coating of Si nanoparticles significantly improved the anode stability, leading to a capacity retention of 94% after 20 cycles (Figure 5a). Furthermore, the small capacity fade might be partially related to the degradation of Li surface resistance during cycling.

In comparison, Si anodes with either Na-CMC (Figure 5b) or PVDF (Figure 5c) binders showed immediate degradation

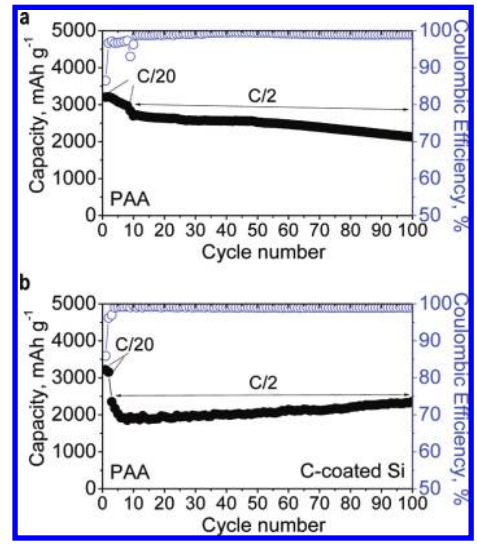

FIGURE 6. Reversible Li deintercalation capacity and Coulombic efficiency of the Si-based anodes with a PAA binder using: (a) as-received Si nanopowder and (b) carbon-coated Si nanopowder. The measurements were performed at room temperature in two-electrode 2016 coin-type half-cells. Si:C = 1:1. Capacity reported for Si part of the anode only.

and not even a few stable cycles in similar experiments. Carbon coatings somewhat improved their stability as well, although the overall anode degradation rates were significantly higher: 42 and 58% capacity retention after 20 cycles in the case of Na-CMC binder (bare Si and C-coated Si); 13% and 16% capacity retention after 20 cycles in the case of PVDF binder (bare Si and C-coated Si). In spite of the small Si particle size, the CE for Si anodes with PAA and Na-CMC binders at the first cycle was in excess of 90% (Figure 5). Even though the irreversible capacity losses could be as high as 340 mA h/g, the high Si capacity minimized the relative value of these losses. The average value of the CE over the first 20 cycles was the highest for C-coated Si with PAA binder, ∼ 97% (Figure 5a). A more efficient electrode dehumidification procedure should be employed to further reduce the irreversible capacity losses.

As a proof-of-concept for the applicability of PAA binders for the long-term charge discharge cycling, we have produced similar anodes but added VC into the electrolyte solution in order to minimize surface polarization on the Li foil counter electrode in our two-electrode tests and improve the solid electrolyte interphase (SEI) layer on the Si anode. The content of the PAA binder was kept low at 15 wt %. The cycling protocol was slightly different for as-received nanoSi (Figure 6a) and C-coated nanoSi (Figure 6b). In the former case, the first ten cycles were performed at the current rate of *C*/20 and the next 90 cycles at the current rate of *C*/2. In the later case, we only performed two cycles at *C*/20 and the next 98 cycles at the current rate of *C*/2. Figure 6a shows that even without carbon coating, Si anodes with PAA binder demonstrate quite stable performance for 100 cycles with less than 0.2% degradation per cycle at a rather fast rate of *C*/2. The average value of the CE was 96.5 for cycles 2−10 (*C*/20) and 99.1 for cycles 11−100 (*C*/2). Higher CE value observed in these tests (compare Figures 5a and 6a) could be related to both the addition of VC into

the electrolyte and lowering the volume expansion due to lower specific capacitance achieved at a faster rate. The formation of C coating on the Si surface decreased the electrode kinetics. Indeed, increasing the current rate by 10 times lowered the specific capacitance by about 1/4 (Figure 6b). Interestingly, after the fifth cycle, the specific capacitance of C-coated Si started to steadily increase and reach 2400 mA h/g after 100 cycles (Figure 6b), suggesting that the kinetics of Li insertion/extraction in to the anode was improving with cycling. Overall, the long-term testing results show very promising potential for the use of PAA binders in Si anodes. We are unfamiliar with any reports on any binder that permitted similar performance of Si anodes when present in comparable quantities (15%) and tested under 100% DoD.

When compared to poorly performing PVDF, the superior performance of both PAA and CMC binders correlates very well with their little-to-no interaction with electrolyte solvent (Figure 2) and their high elastic modulus when immersed in electrolyte (Figure 3). We therefore propose that the rigid structure of a binder and the lack of its interaction with solvent molecules are required for good performance of Si anodes. The lack of PAA and CMC expandability does not constitute an obvious drawback when used in Si anodes. Future work with PAA-based binders having the same surface groups but having different elastic properties will be conducted in order to systematically investigate the impact of the binder elasticity.

Because the mechanical properties and active functional groups of PAA and Na-CMC are similar, we conclude that the high concentration of functional (carboxylic) groups in PVA (PAA) is probably a major cause for its superior performance. We suppose that a certain fraction of the COOH groups in PAA form strong hydrogen bonds with OH groups on the Si (or C) surface. The remaining carboxy groups form ionically conductive COOLi groups and, together with the solid electrolyte interphase (SEI) formed during the first Li insertion, protect the Si—C interface and thus the anode electrical connectivity from degradation upon solvent intercalation.

Further improvements in the Si/PVA-based binder anode should be aimed to (a) allow the formation of a stable yet deformable SEI on the elastic binder-coated Si surface (the elasticity of a polymer matrix may prevent cracking in SEI upon the volume changes) and (b) sustain repeated cycling without failure while maintaining electrical conductivity within the anode.

CONCLUSION

In conclusion, we have demonstrated for the first time that pure PAA may serve as an effective binder for Si-based Li-ion battery anodes. Similarly to Na-CMC, this binder shows low swellability in carbonates and a high elastic modulus. However, PAA's higher concentration of carboxylic groups is suggested to affect its performance favorably. Carbon coatings on the surface of Si nanoparticles have been found to improve the stability for all the binders studied. At the C/2 current rate, the C-coated Si anodes with PAA binders demonstrated stable performance for more than 100 cycles and Coulombic efficiency in excess of 99%. Further improvements in the binder properties may allow further enhancements in the SEI stability.

Acknowledgment. This work was supported by NASA via Contract No. NNC08CB01C. Huebner was supported by the National Science Foundation under Grant No. EEC-0946373 to the American Society for Engineering Education.

REFERENCES AND NOTES

(1) Poizot, P.; Laruelle, S.; Grugeon, S.; Dupont, L.; Tarascon, J. M. *J. Power Sources* **2001**, *97—8*, 235–239.
(2) Wilson, A. M.; Reimers, J. N.; Fuller, E. W.; Dahn, J. R. *Solid State Ionics* **1994**, *74*, 249–254.
(3) Beaulieu, L. Y.; Hatchard, T. D.; Bonakdarpour, A.; Fleischauer, M. D.; Dahn, J. R. *J. Electrochem. Soc.* **2003**, *150*, A1457–A1464.
(4) Magasinski, A.; Dixon, P.; Hertzberg, B.; Kvit, A.; Ayala, J.; Yushin, G. *Nat. Mater.* **2010**, *9*, 353–358.
(5) Hertzberg, B.; Alexeev, A.; Yushin, G. *J. Am. Chem. Soc.* **2010**, *132*, 8548–8549.
(6) Kang, Y. M.; Go, J. Y.; Lee, S. M.; Choi, W. U. *Electrochem. Commun.* **2007**, *9*, 1276–1281.
(7) Shim, J.; Kostecki, R.; Richardson, T.; Song, X.; Striebel, K. A. *J. Power Sources* **2002**, *112*, 222–230.
(8) Kim, I.; Kumta, P. N.; Blomgren, G. E. *Electrochem. Solid-State Lett.* **2000**, *3*, 493–496.
(9) Kim, I. S.; Kumta, P. N. *J. Power Sources* **2004**, *136*, 145–149.
(10) Chen, L. B.; Xie, X. H.; Xie, J. Y.; Wang, K.; Yang, J. *J. Appl. Electrochem.* **2006**, *36*, 1099–1104.
(11) Liu, W. R.; Yang, M. H.; Wu, H. C.; Chiao, S. M.; Wu, N. L. *Electrochem. Solid-State Lett.* **2005**, *8*, A100–A103.
(12) Buqa, H.; Holzapfel, M.; Krumeich, F.; Veit, C.; Novak, P. *J. Power Sources* **2006**, *161*, 617–622.
(13) Li, J.; Lewis, R. B.; Dahn, J. R. *Electrochem. Solid-State Lett.* **2007**, *10*, A17–A20.
(14) Beattie, S. D.; Larcher, D.; Morcrette, M.; Simon, B.; Tarascon, J. M. *J. Electrochem. Soc.* **2008**, *155*, A158–A163.
(15) Mazouzi, D.; Lestriez, B.; Roue, L.; Guyomard, D. *Electrochem. Solid-State Lett.* **2009**, *12*, A215–A218.
(16) Li, J.; Christensen, L.; Obrovac, M. N.; Hewitt, K. C.; Dahn, J. R. *J. Electrochem. Soc.* **2008**, *155*, A234–A238.
(17) Chen, Z. H.; Christensen, L.; Dahn, J. R. *Electrochem. Commun.* **2003**, *5*, 919–923.
(18) Key, B.; Bhattacharyya, R.; Morcrette, M.; Seznec, V.; Tarascon, J. M.; Grey, C. P. *J. Am. Chem. Soc.* **2009**, *131*, 9239–9249.
(19) Bridel, J. S.; Azais, T.; Morcrette, M.; Tarascon, J. M.; Larcher, D. *Chem. Mater.* **2010**, *22*, 1229–1241.
(20) Guo, J. C.; Wang, C. S. *Chem. Commun.* **2010**, *46*, 1428–1430.
(21) Ui, K.; Kikuchi, S.; Mikami, F.; Kadoma, Y.; Kumagai, N. *J. Power Sources* **2007**, *173*, 518–521.
(22) Li, J.; Le, D. B.; Ferguson, P. P.; Dahn, J. R. *Electrochim. Acta* **2010**, *55*, 2991–2995.
(23) J. Brandrup, E. H. I., Grulke, E. A., *Polymer Handbook*. 4th ed.; John Wiley & Sons, Inc: New-York, 1999.
(24) Luzinov, I.; Julthongpiput, D.; Bloom, P. D.; Sheares, V. V.; Tsukruk, V. V. *Macromol. Symp.* **2001**, *167*, 227–242.
(25) Fan, X. D.; Hsieh, Y. L.; Krochta, J. M.; Kurth, M. J. *J. Appl. Polym. Sci.* **2001**, *82*, 1921–1927.
(26) Antonova, N. M. *Russ. J. Non-Ferrous Met.* **2009**, *50*, 419–423.
(27) Liu, Z. H.; Marechal, P.; Jerome, R. *Polymer* **1998**, *39*, 1779–1785.
(28) Ager, J. W.; Veirs, D. K.; Rosenblatt, G. M. *Phys. Rev. B* **1991**, *43*, 6491–6499.
(29) Chan, C. K.; Ruffo, R.; Hong, S. S.; Huggins, R. A.; Cui, Y. *J. Power Sources* **2009**, 34–39.
(30) Obrovac, M. N.; Krause, L. J. *J. Electrochem. Soc.* **2007**, *154*, A103–A108.
(31) Li, J.; Dahn, J. R. *J. Electrochem. Soc.* **2007**, *154*, A156–A161.